OPTIMAL CONTROLLER DESIGN FOR MORE-ELECTRIC AIRCRAFT POWER SYSTEMS

by

Sinan Yigit

BS, TOBB University of Economics and Technology, 2011

Submitted to the Graduate Faculty of

Swanson School of Engineering in partial fulfillment

of the requirements for the degree of

Master of Science

University of Pittsburgh

2014

UNIVERSITY OF PITTSBURGH

SWANSON SCHOOL OF ENGINEERING

This thesis was presented

by

Sinan Yigit

It was defended on

July 23, 2014

and approved by

Zhi-Hong Mao, Ph.D., Associate Professor, Department of Electrical and Computer Engineering

Gregory Reed, Ph.D., Professor, Department of Electrical and Computer Engineering

Thomas McDermott, Ph.D., Assistant Professor, Department of Electrical and Computer Engineering

Ervin Sejdić, Ph.D., Assistant Professor, Department of Electrical and Computer Engineering

Thesis Advisor: Zhi-Hong Mao, Ph.D., Associate Professor, Department of Electrical and Computer Engineering

Co-Advisor: Gregory Reed, Ph.D., Professor, Department of Electrical and Computer Engineering

OPTIMAL CONTROLLER DESIGN FOR MORE-ELECTRIC AIRCRAFT POWER SYSTEMS

Sinan Yigit, M.S.

University of Pittsburgh, 2014

Electrical energy is becoming more and more popular these days. Because energy efficiency has always been an important aspect for human kind, the vehicles which use energy efficiently are more preferable. The rapid changes in the technology allow us to build more electric systems such as more electric aircraft (MEA). The MEA concept is a major trend in today's world, but building those vehicles faces some challenges. The subsystems of MEA which consume electricity rather than other energy sources might increase electrical loads of power electronic converters and motor drive systems. Motor drive systems and power electronic systems generally have characteristics of constant power loads (CPL). In small-signal analysis, CPL presents negative impedance that might deteriorate the power system stability margin. This thesis aims to model a typical MEA power system and design an optimal controller which is able to solve the stability issue with CPL. The dynamic model is derived using the equivalent circuit model and linearization around an operating point. This optimal control method provides a solution, which is optimal with respect to a quadratic performance index. MATLAB is used to solve algebraic Riccati equation and obtain figures for the simulation. When it is compared to the effect of conventional power system stabilizers (PSS), the proposed Linear Quadratic Regulator (LQR) gives more robust results. Moreover, the state feedback gain is calculated only for one operating point, but it works over wide range of operating conditions.

TABLE OF CONTENTS

LIST OF TABLES

LIST OF FIGURES

ACKNOWLEDGEMENT

I would like to express my deepest and sincere gratitude to both of my advisors, Dr. Zhi-Hong Mao and Dr. Gregory Reed for their guidance and invaluable help throughout the course of this research. I also would like to thank Shimeng Huang and Qin-hao Zhang for their valuable assistance to me in this study.

Thanks are also due to all my friends and colleagues in the Power Engineering research group for their continuous support and valuable discussions during my time in the school. Thanks to Turkish people who have given me the opportunity of studying by granting me a Ministry of National Education Scholarship. Thanks also to all who have educated me: my primary, secondary and high school teachers, and faculty at TOBB University of Economics and Technology, Turkey.

Finally a million thanks to my father, mother, and Yigit family. I learned a lot from them. Without their encouragement, understanding and love, it would be impossible to finish my study.

1.0 INTRODUCTION

Since the regulations to protect the environment, and concerns about energy efficiency and energy cost are increasing "more electrical" vehicle concept is becoming more and more popular [1]. As one of them the more-electric aircraft is a recent development which is mostly related to the electrical power system (EPS) of an aircraft. However this cutting-edge development boosted up the electrical loads based on power electronic converter and motor drive systems. These electrical loads which are regulated by power electronic devices generally tend to have constant power load (CPL) characteristics. In AC systems the loads generally have positive incremental impedance characteristic. Since the voltage and the current increases or decreases at the same time in these systems the impedance doesn't have negative values. Contrarily, the ripples on the CPLs have negative impedance because when the voltage increases the current is decreased or vice versa. In Figure 1. the comparison of positive and negative incremental impedance characteristics is shown. As seen from the figure when the source voltage is increased the resistive load voltage decreases. Besides that, even though the source voltage is reduced the CPL voltage decays. This phenomenon has a huge effect on narrowing the stability margin of power system [2]. It is generally related to tightly regulated loads that drive the motor in the electric power system.

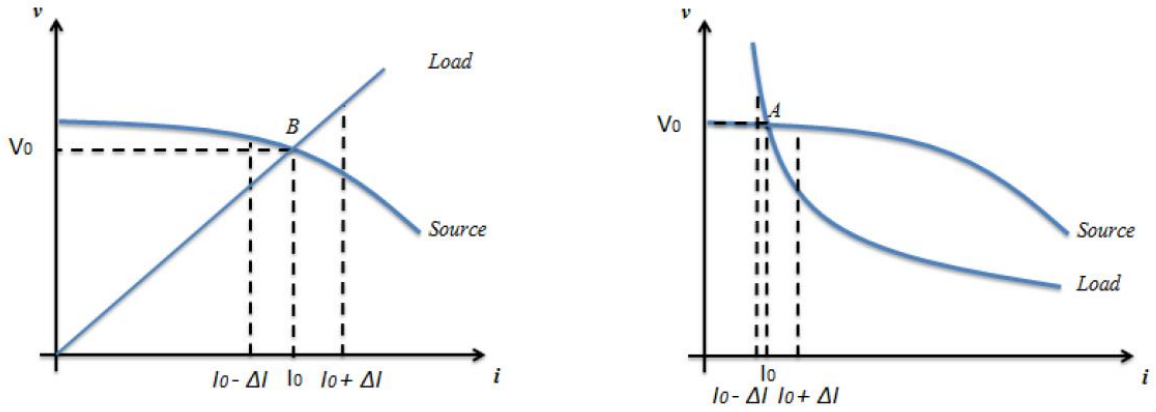

Figure 1. Resistive Load (Left) vs CPL (Right) (Adapted from [10])

As mentioned earlier the more electric aircraft has motor drive systems and power electronic loads. Since these loads cause negative impedance to extend the stability margin it is necessary to develop appropriate models. Therefore these models enable the researchers to show the dynamical characteristics of aircraft EPS. There are several studies have been carried out [1, 2, 3] but unfortunately the generalized solution couldn't be come out.

1.1 LITERATURE REVIEW

The goal of this study is to find the stability constraints of an aircraft electrical power system and to apply an appropriate control method by tuning the controller parameters to extend these constraints. In this study the model consists of an AC generator, three-phase controlled rectifier, and dynamical constant power load.

Since the main purpose is to extend the stability margin it is thought to choose one of the optimal control methods. Linear Quadratic Regulator (LQR) will be used as an optimal control

method. This method will enhance the stability margin of the system substantially but this study is strictly theoretical. Because of that it won't give a chance to specify the new certain limits for the stability.

Power electronic devices are used in lots of systems or subsystems such as motor drive systems [2]. compensators on transmission lines [4], telecommunication systems [5]. vehicles [6]. and industrial power systems [7]. The load of those systems can be pure resistive, pure inductive, a constant source, combination of those. Besides that CPL can be come across in one of those systems. As stated before motor drive systems' tight regulation causes electric loads have negative impedance characteristics.

Some studies have been carried out to understand the stability behavior of the CPL. However as mentioned previously there is no general solution to enhance stability of such a system. Figure 2. shows a rectifier and a constant power load.

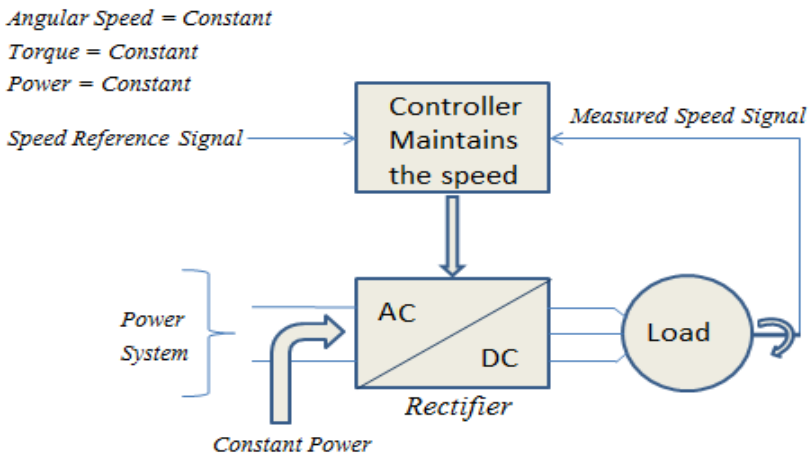

Figure 2. Controlled Rectifier and Constant Power Load (Adapted from **[10]**)

1.2 AIRCRAFT AC ELECTRICAL POWER SYSTEM ARCHITECTURE

Recent studies related to MEA power system stability aimed to implement electromechanical actuators instead of using the hydraulic and air actuators. To be able to realize implementation of those actuators, the researchers tried to find better ways to generate large amount of power in a reliable way.

As stated in the first chapter, power electronic devices gives an opportunity to the researchers to generate appropriate frequency, current, or voltage. Older power systems require conventional electric power equipment such as circuit breakers. However, recent technology which uses power electronic converters enables us to manage power system in a more accurate and reliable way. On the other hand, recent technology provides robust and fast control applications to the engineers who work in that area.

Figure 3. represents a transport aircraft electric power system architecture. It consists of batteries, generators, rectifiers, inverters, dc-dc converters, control units, and electromechanical and electrohydrostatic actuators.

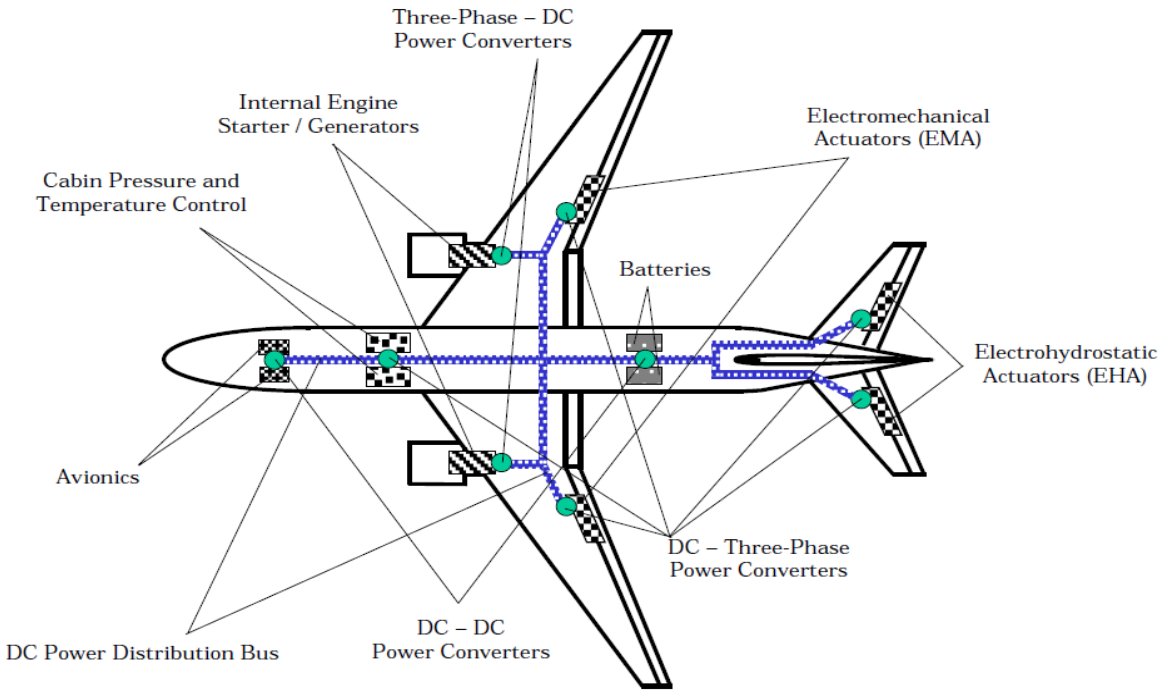

Figure 3. Power distribution system of a transport aircraft (Adapted from [8])

Some parts of this electric power system operates in regenerative mode. In general, the electric power is transmitted from the generators to the loads. In regenerative mode specific loads may provide electric power to the loads. This operation mode contributes to energy efficiency. For instance, the battery can be used as an energy source and the auxiliary power unit generator functions as a motor to start the engine [8]. Therefore it gives some advantages such as storage of power for future usage. In contrast, some voltage fluctuations may occur because of unused regenerative power. Control unit is able to regulate these fluctuations.

The block diagram of the power distribution system is shown in Figure 4. [8]

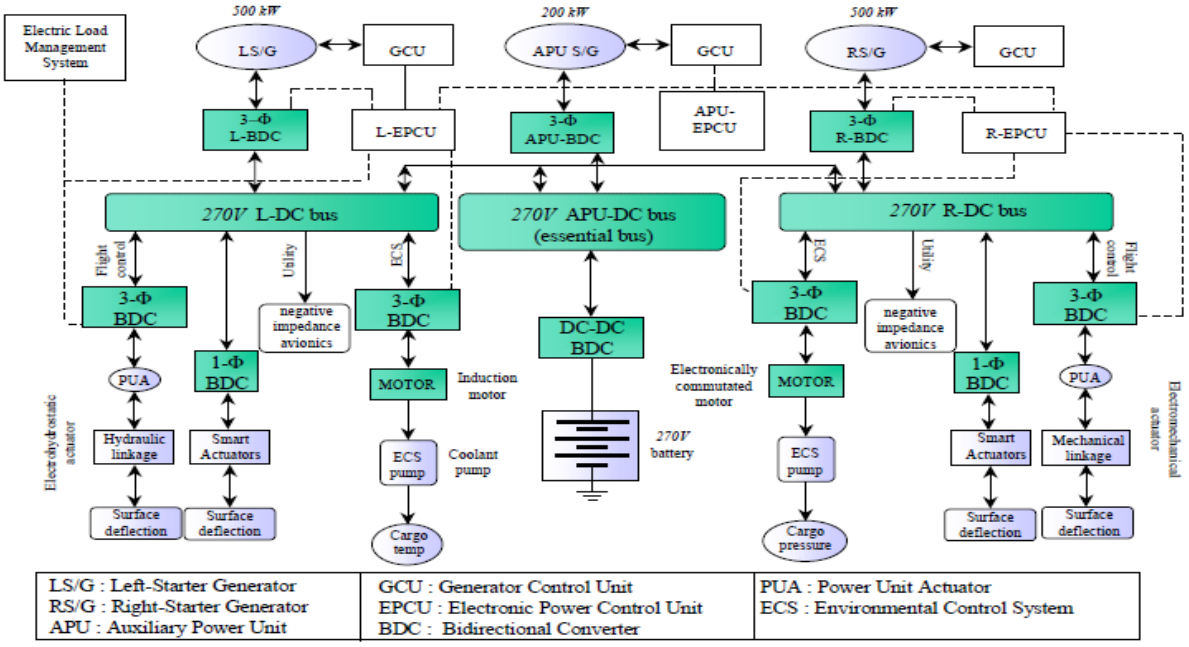

Figure 4. Power Distribution System Diagram (Adapted from [8])

As seen from the diagram (Figure 4.) the system architecture is very complicated. It increases the amount of parameters needed to be taken into account. Therefore simplification of the model is necessary to facilitate the stability problem. The proposed model consists of an AC source, rectifier, constant power load (CPL).

2.0 MODELING OF THE MEA POWER SYSTEM

2.1 POWER SYSTEM DEFINITION

Before generating the general model it might be beneficial to understand large-signal and small-signal definitions. Equation (2.1) and (2.2) represents AC and DC terms around an operating point.

$$i_0 = I_0 + \tilde{\imath}_0 \tag{2.1}$$

$$v_0 = V_0 + \tilde{v}_0 \, . \tag{2.2}$$

In these equations the DC terms are represented by the capital letters while the small perturbations are shown as $\tilde{\imath}_0$ and $\tilde{v}_0$. Furthermore the expressions for the current and voltage depending on time are as follows: [9]

$$v(t) = V_{max}.\cos(\omega t) \tag{2.3}$$

$$i(t) = I_{max}.\cos(\omega t - \alpha) \, . \tag{2.4}$$

By substituting equation 2.1 and 2.2 into those equations the expression for the constant power can be written as:

$$P = \frac{1}{2}(V_{max} + \tilde{\mathrm{V}}_{max})(I_{max} + \tilde{\mathrm{I}}_{max}).\cos(\alpha) \, . \tag{2.5}$$

Since it is constant the equation 2.5 is equal to:

$$P = \frac{1}{2}V_{max}I_{max}.\cos(\alpha) \, . \tag{2.6}$$

If the second order terms are neglected:

$$\frac{\tilde{V}_{max}}{\tilde{I}_{max}} = \frac{V_{max}}{I_{max}} = -R_{CPL} \, . \tag{2.7}$$

Equation 2.7 shows that the small signal model of the AC CPL behaves as a negative impedance.

Figure 5. depicts large-signal and small-signal model of a constant power load. [10]

Figure 5. Large-signal (left) and small-signal (right) model of CPL

2.2 MODELING OF SUBSYSTEMS

It is necessary to introduce the models of subsystems. These subsystems are as follows:

1. Rectifier Model
2. Electromechanical Actuator Model
3. Ideal Constant Power Load

2.2.1 Rectifier Model

To make the problem easier the converter is assumed to be operating under the continuous-conduction mode (CCM). Besides that the A, B, C phases are thought to be balanced. The following figure shows a CPL with 3-phase diode rectifier.

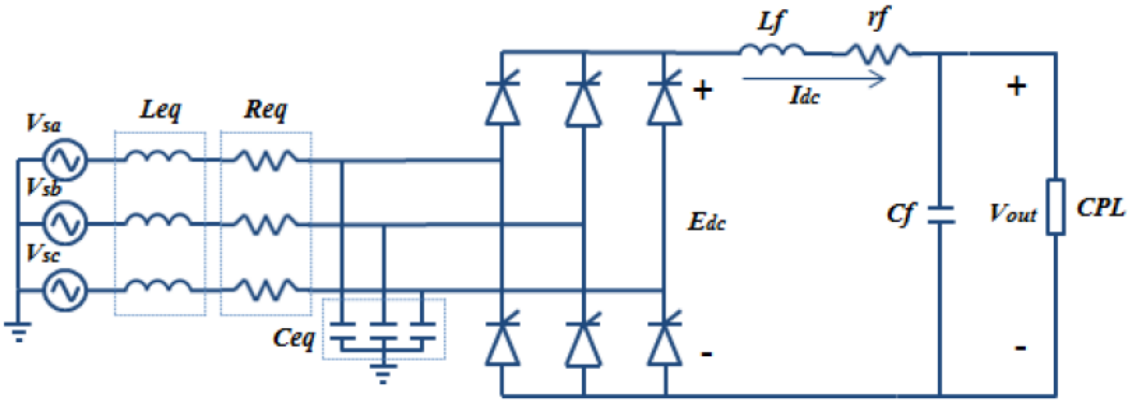

Figure 6. CPL with 3-phase Diode Rectifier

For convenience the rectifier part can be modeled as a transformer. Therefore the mathematical expression of the combined system can be much easier. Since the equivalent inductance (L_{eq}) in Figure 6. stores current and releases it by time it may result voltage drop on the DC side. This might cause an overlap angle because of charging and discharging of the current. [11] To represent this voltage drop the R_{μ} resistance is placed on the DC side and it depends on ω and equivalent inductance on the AC side.

2.2.2 Electromechanical Actuator Model

To be able to model electromechanical actuators (EMA) it is necessary to construct the model of AC machine and choose the controller of the EMA. As mentioned earlier the controller in this study is linear quadratic regulator because it can be easily implemented and it is robust. Additionally, other studies related to CPL phenomenon used PI controller because it is very common in the industry.

First, to construct the motor model the following concepts need to be understood. The definition of the parameters In an AC motor can be found in Appendix-B.

By using the definitions in Appendix-B the phase currents can be expressed as:

$$i_a = I_m \cos(\omega t) \tag{2.7}$$

$$i_b = I_m \cos\left(\omega t - \frac{2\pi}{3}\right) \tag{2.8}$$

$$i_c = I_m \cos\left(\omega t + \tfrac{2\pi}{3}\right). \tag{2.9}$$

Currents of the each phase will provide a magneto-motive force (MMF). The following equations show the MMFs which are generated by each phase current:

$$F_a(\theta) = N i_a \cos(\theta) \tag{2.10}$$

$$F_b(\theta) = N i_b \cos\left(\theta - \frac{2\pi}{3}\right) \tag{2.11}$$

$$F_c(\theta) = N i_c \cos\left(\theta + \tfrac{2\pi}{3}\right). \tag{2.12}$$

Then the overall MMF can be written as:

$$F(\theta) = F_a(\theta) + F_b(\theta) + F_c(\theta)$$

$$= Ni_a \cos(\theta) + Ni_b \cos\left(\theta - \tfrac{2\pi}{3}\right) + Ni_c \cos\left(\theta + \tfrac{2\pi}{3}\right). \quad (2.13)$$

Substituting 2.7, 2.8 and 2.9 yields: [12]

$$F(\theta, t) = NI_m[\cos(\omega t)\cos(\theta) + \cos\left(\omega t - \frac{2\pi}{3}\right)\cos\left(\theta - \frac{2\pi}{3}\right)$$

$$+ \cos\left(\omega t + \frac{2\pi}{3}\right)\cos\left(\theta + \frac{2\pi}{3}\right)]$$

$$= \tfrac{3}{2} NI_m \cos(\omega t - \theta). \quad (2.14)$$

The rotation of the rotor is provided by this magnetic force. As an AC motor PM machine is chosen in this study. Induction machines (Asynchronous machines) has field windings on its rotor. On the other hand, permanent magnet synchronous machines (PMSM) use permanent magnets as the rotating part. PMSMs have some advantages over induction machines (IM): [12]

*They eliminate field copper loss since they don't use windings on the rotor.

*They have higher power density because of permanent magnets.

*Their rotor inertia is also lower than the one of IMs.

*PMSMs are much more efficient than IMs. However their prices are much higher than IMs.

To simplify the problem the PMSM is assumed to be generating constant flux. It means the system provides pure reactive power. Therefore the real power dynamics are neglected.

The relationship between the input current and input voltage is as follows:

$$V_{in} = R_m I_{in} + \omega F_m + L_f \dot{I}_{in}. \quad (2.15)$$

The rotor instantaneous speed can be written as:

$$\omega^* = \frac{P}{2}\omega_r. \tag{2.16}$$

According to Newton's law the torque-speed relation is as follows: [12]

$$J_m\dot{\omega}_r = K_T I_{CPL} - T_L. \tag{2.17}$$

The torque constant can be expresses as:

$$K_T = \frac{3}{2}\frac{P}{2}F_m. \tag{2.18}$$

The block diagram for the relationship of current and voltage through EMA which is obtained by using equation 2.15, 2.16, 2.17, 2.18 is represented in Figure 7.

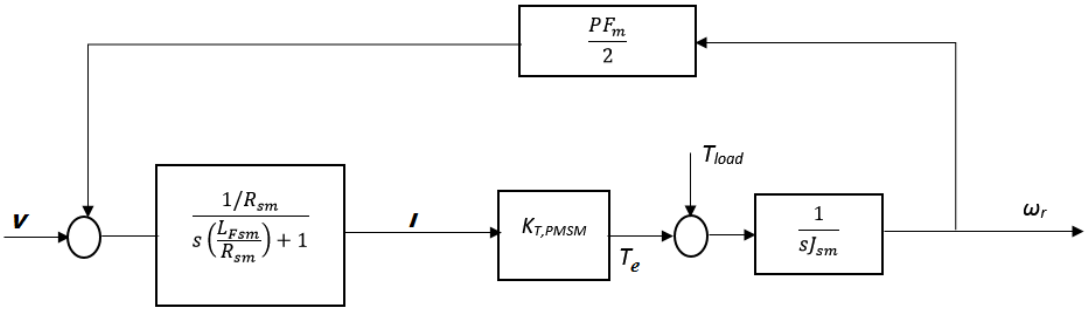

Figure 7. Voltage – Current relationship of the permanent magnet synchronous machine (Adapted from [3])

2.2.3 Ideal Constant Power Load

As stated in the first section when motor drives and power converters is controlled tightly, they intend to cause negative impedance. It is the nature of CPL. To clarify this point, if the load torque

and angular velocity of the motor is kept constant, the power of the motor won't change during that time. Therefore it will affect the stability of the system in a bad way. Figure 8. shows a CPL through a low-pass filter (LPF).

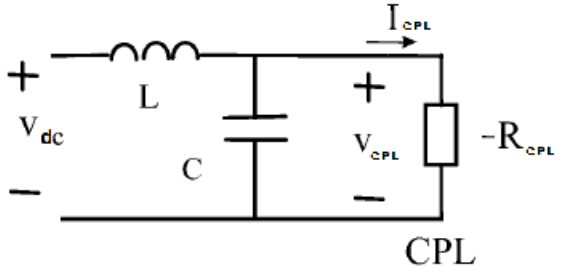

Figure 8. Generalized model for a CPL

Let's consider a small increase on the current I_{CPL}. It will result in a small reduction on voltage V_{CPL} because of negative impedance characteristic of CPL. It is necessary to look at the characteristic equation of the generalized CPL model to observe stability issue. The transfer function of the model in Figure 8. is as follows:

$$\frac{V_{CPL}}{V_{dc}} = \frac{V_{dc}.(\frac{1}{sC}||(-R_{CPL}))}{sL + (\frac{1}{sC}||(-R_{CPL}))} \tag{2.19}$$

$$\frac{V_{CPL}}{V_{dc}} = \frac{R_{CPL}}{s^2CLR_{CPL} - sL}. \tag{2.20}$$

As seen from equation (2.29) the denominator of the dynamical equation has one positive and one negative poles. Because of the positive pole the CPL system is not stable and if a controller is not used the system will suffer from instability issue. The CPL can be thought as an ideal voltage

dependent current source. **Error! Reference source not found.** Therefore it can be said that it oesn't have any dynamical behavior. However when the EMA is involved into the system CPL begins to deviate from the ideal situation.

2.3 EQUIVALENT MODEL OF THE OVERALL SYSTEM

Since the parts of the studied system is analyzed in previous sections overall system can be obtained by combining the subsystems. As stated in first chapter the proposed model (Figure 9.) consists of an AC source model, rectifier model, and CPL model (EMA).

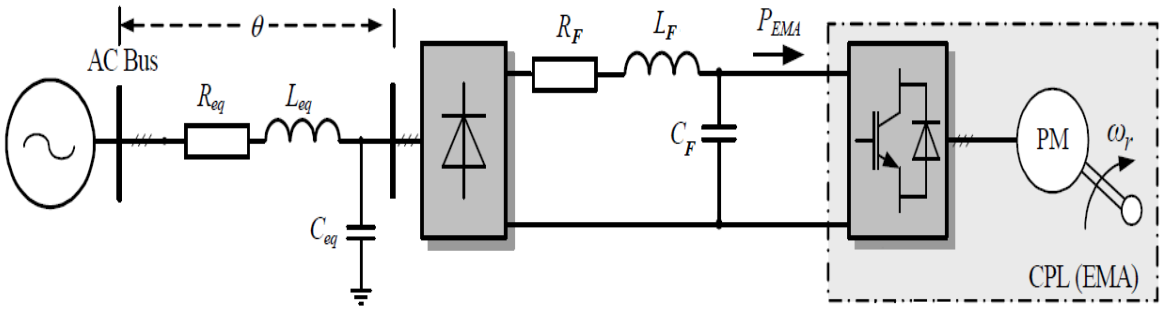

Figure 9. Three-phase power system model (Adapted from **Error! Reference source not found.**)

To obtain the differential equations it might be good to simplify the model. If the CPL model is thought as one block which has an input current and voltage between two nodes, the equivalent model of hybrid power system can be represented as in Figure 10. Since CPL consumes constant power it is necessary to regulate i_o and v_o.

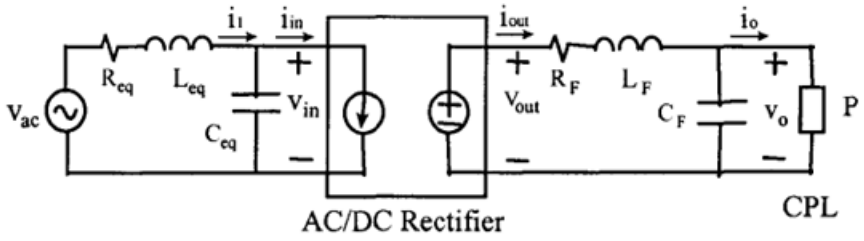

Figure 10. Equivalent model of one-phase power system (Adapted from [1])

While *u(t)* is the commutation function of the rectifier (Figure 11.). i_{in} and v_{out} can be defined as follows: [9]

$$i_{in} = u(t).i_{out} \tag{2.21}$$

$$v_{out} = u(t).v_{in}\ . \tag{2.22}$$

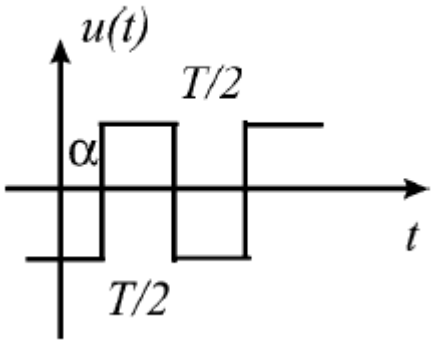

Figure 11. Commutation function of the rectifier (Adapted from [9])

Voltage and current relations of the circuit can be expressed as: [1]

$$v_{ac} = R_{eq}.i_1 + L_{eq}.\frac{di_1}{dt} + v_{in} \tag{2.23}$$

$$C_{eq}.\frac{dv_{in}}{dt} + i_{in} = i_1 \tag{2.24}$$

$$v_{out} = R_F.i_{out} + L_F.\frac{di_{out}}{dt} + v_o \tag{2.25}$$

$$C_F.\frac{dv_o}{dt} + \frac{P}{v_o} + \frac{v_o}{R} = i_{out}\ . \tag{2.26}$$

Through equations 21-26 of the system model it is possible to obtain the actual state-space variables by separating the imaginary and real parts. Therefore, the harmonic terms of the circuit state variables correspond to those first and zero harmonic terms. These state variables can be expressed as i_1, v_{in}, i_{out}, and v_o. Furthermore, to obtain state space matrices first-order approximation can be used. Because of the first and zero order term 12 real state variables will be provided as follows: [9]

Zero harmonic terms:

$$< i_1 >_0 = x_1 \tag{2.27}$$

$$< v_{in} >_0 = x_2 \tag{2.28}$$

$$< i_{out} >_0 = x_3 \tag{2.29}$$

$$< v_o >_0 = x_4\ . \tag{2.30}$$

First harmonic terms:

$$< i_1 >_1 = x_5 + jx_6 \tag{2.31}$$

$$< v_{in} >_1 = x_7 + jx_8 \tag{2.32}$$

$$< i_{out} >_1 = x_9 + jx_{10} \tag{2.33}$$

$$< v_o >_1 = x_{11} + jx_{12}\ . \tag{2.34}$$

When the AC source is assumed to be sinusoidal the equations for first and zero harmonic terms of the source can be written as:

$$< v_{ac} >_0 = 0 \tag{2.35}$$

$$< v_{ac} >_1 = -j\frac{V_m}{2}. \tag{2.36}$$

Since CPL has nonlinear characteristics the generalized state-space average model is nonlinear. The voltage deviations are assumed to be low when they are compared to DC value of v_o. Then first and zero harmonics of the inverse of output voltage are as follows: [1]

$$< \frac{1}{v_o} >_0 = \frac{1}{x_4}. \tag{2.37}$$

$$< \frac{1}{v_o} >_1 = -\frac{x_{11}}{{x_4}^2} - j\frac{x_{12}}{{x_4}^2}. \tag{2.38}$$

2.3.1 DQ Transformation of the Studied Model

So far the simplified system was one-phase system and its differential equations and state space representations are obtained accordingly. However power distribution systems in modern aircrafts are generally three-phase and it is necessary to take this phenomenon into account.

Now it makes sense to use Park's (dq0) transformation to simplify the model and make the real and reactive power expressions apart from each other for ease of calculation. Assuming a three-phase balanced system the following gives the vector representation from a, b, and c phases to dq rotating coordinate systems after normalization: [29]

$$[d_u \quad q_u \quad 0_u] = [a_u \quad b_u \quad c_u]\begin{bmatrix} cos\theta & -sin\theta & \frac{1}{2} \\ \cos(\theta - \frac{2\pi}{3}) & -\sin(\theta - \frac{2\pi}{3}) & \frac{1}{2} \\ \cos(\theta + \frac{2\pi}{3}) & -\sin(\theta + \frac{2\pi}{3}) & \frac{1}{2} \end{bmatrix}. \tag{2.40}$$

Where $\boldsymbol{\theta}$ represents the rotating angle and is equal to $\boldsymbol{\omega t}$. Because of the balanced three-base system after transformation zero component isn't used for simplification. 'd' stands for the direct axis; and 'q' for quadrature axis. The q-axis is perpendicular to the direct axis. Figure 12. represents the transformation geometrically.

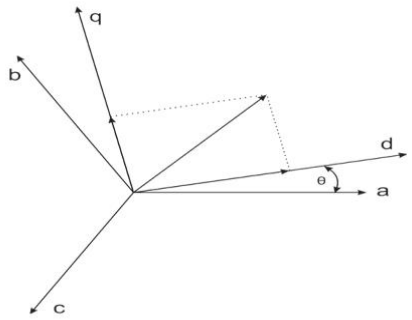

Figure 12. abc to dq0 Transformation

Referencing Figure 12. the model of studied system can be transformed onto dq coordinate plane. After transformation the new model is shown in Figure 13.

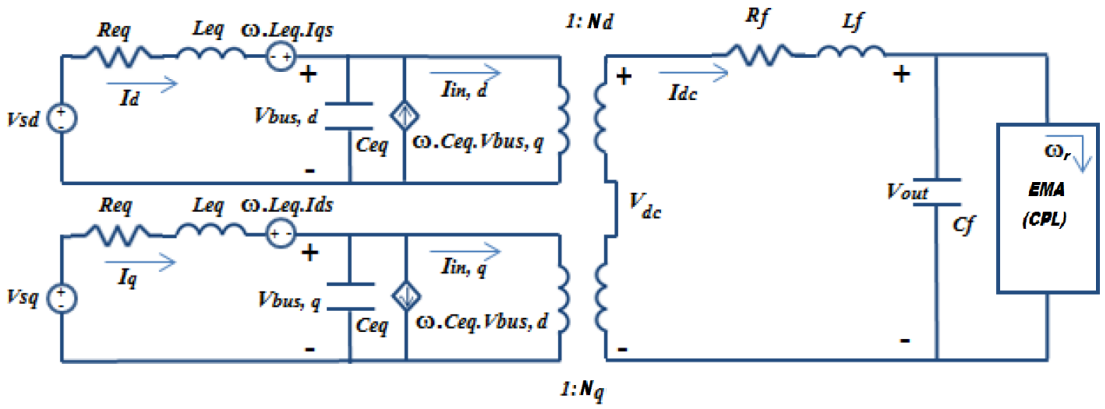

Figure 13. dq transformation of the studied model (Adapted from [10])

Next step is to simplify the complete model by fixing the rotating frame on the phase of the switching function, represented in the equation. Moreover, it is assumed to provide pure reactive power to the synchronous machine. Figure 14 shows the simplified version of the studied model.

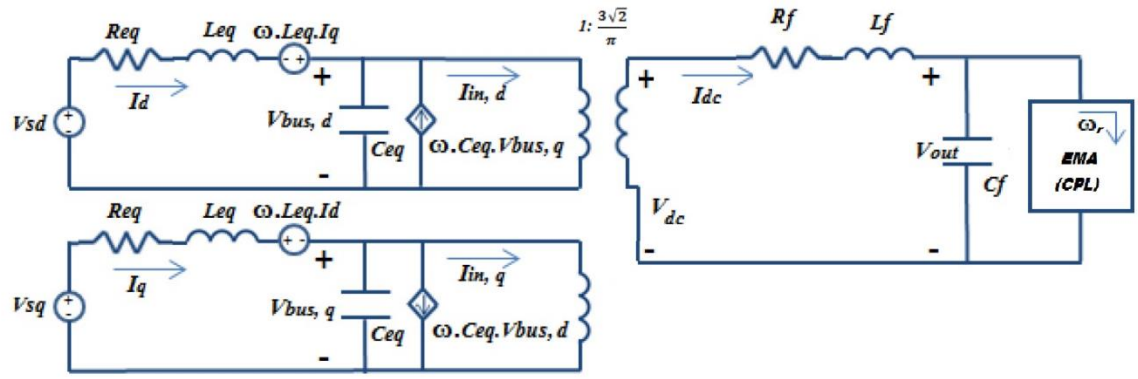

Figure 14. Simplified block diagram of the model after transformation (Adapted from [10])

In Figure 15. the EMA block is shown:

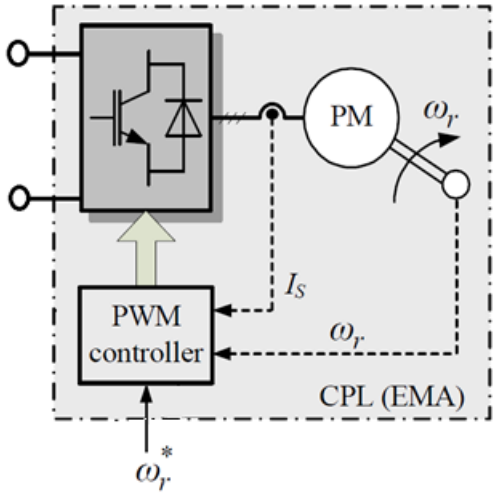

Figure 15. EMA block in Figure 14 (Adapted from [12])

After that the differential equations according to those block diagrams can be shown as follows:

$$L_{eq}\dot{I}_d = -R_{eq}I_d + L_{eq}\omega I_q - V_{bus,d} + V_{sd} \tag{2.41}$$

$$L_{eq}\dot{I}_q = -R_{eq}I_q - L_{eq}\omega I_d - V_{bus,q} + V_{sq} \tag{2.42}$$

$$C_{eq}\dot{V}_{bus,d} = I_d + C_{eq}\omega V_{bus,q} - \left(\frac{3\sqrt{2}}{\pi}\right)I_{dc} \tag{2.43}$$

$$C_{eq}\dot{V}_{bus,q} = -C_{eq}\omega V_{bus,d} + I_q \tag{2.44}$$

$$L_F\dot{I}_{dc} = \left(\frac{3\sqrt{2}}{\pi}\right)V_{bus,d} + R_F I_{dc} - V_{dc} \tag{2.45}$$

$$C_F\dot{V}_{dc} = I_{dc} - \frac{P_{cpl}}{V_{out}} \tag{2.46}$$

$$L_{sm}\dot{I}_s = -\frac{PF_m\omega_r}{2} - R_{sm}I_s + V_{dc} \tag{2.47}$$

$$J_m\dot{\omega}_r = K_T I_{dc} - T_{load}\,. \tag{2.48}$$

Where the states are $X=<I_d, I_q, V_{bus,d}, V_{bus,q}, I_{dc}, V_{dc}, I_s, \omega_r>$. The definition of the states is as follows: $I_{d,}$ d-axis current of the source; $I_{q,}$ q-axis current of the source; $V_{bus,d}$, d-axis voltage of the bus; $V_{bus,q}$, q-axis voltage of the bus; I_{dc}, DC current on the rectifier's DC side; V_{dc}, voltage between the rectifier's two nodes; I_{sm}, current of the synchronous machine; ω_r, rotor speed of the synchronous machine. The control is the components of generator voltage in d-axis and q-axis.

3.0 CONTROL METHODOLOGY

As stated in previous chapters this study will use LQR to regulate voltage and current. Main concern of optimal control is to operate a dynamic system at minimum cost. The cost function can be defined as the function of unwanted deviations of the states. Performance index of a continuous time LQR problem is as follows: [16]

$$J(t) = \int_0^\infty (x^T Q x + u^T R u + 2x^T N u) dt \, . \tag{3.1}$$

Where dynamic equations of the system is expressed as:

$$\dot{\mathrm{X}} = AX + Bu \tag{3.2}$$

$$Y = CX \, . \tag{3.3}$$

To define an LQR problem some limitations should be taken into account: [16]

- The system or plant needs to be a linear system.
- The A and B matrices need to be stabilizable and controllable.
- R is symmetric positive definite matrix.
- Q and N are symmetric positive semi-definite matrices.

The solution to that problem is defined as Riccati equation. General formula of the Riccati equation can be shown as:

$$A^T S + SA - (SB + N) R^{-1} (B^T S + N^T) + Q = 0. \, . \tag{3.4}$$

Furthermore, it is hard to solve the equation (3.4) by hand. Therefore MATLAB software is used to solve that equation. Then ***S*** matrix in that equation can be obtained. To be able to get Kalman gain in the following equation the matrices can be substituted:

$$\mathrm{K} = R^{-1}(B^T S + N^T)\ . \tag{3.5}$$

In Figure 11. the control loop is represented where K is the state-feedback or Kalman gain. The input can be found in terms of the optimal gain 'K' and states 'x' by using the following equation:

$$u = -Kx. \tag{3.6}$$

To be able to get a feasible answer for the step response, feed-forward gain 'K_f' should be tuned to make the DC gain equal to zero. Now the input can be defined as follows:

$$u = K_{ff} r_{ref} - KX\ . \tag{3.7}$$

In this study instantaneous value of the CPL voltage 'V_o' is 'r_{ref}' since it needs to be regulated and changes by time. Now the equation (3.5) can be rewritten as:

$$u = K_{ff} V_o^{\ *} - KX\ . \tag{3.8}$$

If equation 3.6 is substituted into equation (3.2): [10]

$$\dot{\mathrm{X}} = AX + B(K_{ff} V_o^{\ *} - KX)\ . \tag{3.9}$$

Then it can expressed as in equation (3.8):

$$\dot{\mathrm{X}} = (A - BK)X + BK_{ff} V_o^{\ *}. \tag{3.10}$$

3.1 INTRODUCTION

One of the most important key requirements for an electric power system is stability. Therefore regulation of current and voltage come into prominence. When negative impedance instability characteristics of a CPL is considered controlling the voltage and the current is of critical importance to provide the stability. [18] Therefore choosing the controller and the tuning the controller parameters are two key factors in this problem. However definition of the problem comes first.

In this study the goal is to find an optimal input '*u*' (voltage value) which corresponds to $K_f V_o - KX$. This optimal input is responsible to minimize performance index '*J*' (deviations from the desired value). Moreover, this performance index is subject to $\dot{X}=AX+B(K_f V_o^{*}-KX)$. In other words, the purpose is to obtain a voltage which minimizes the fluctuations in the studied system. However it is necessary to specify the constraints in terms of state space expressions.

3.2 LINEARIZATION

The LQR system or plant needs to be a linear system. The equations (2.41) – (2.48) represents the nonlinear characteristic of the power system. The equations need to be linearized for small signal analysis. Dynamic equation for the small signal deviations can be written as:

$$\delta\dot{x} = A(x_0, u_0)\delta x + B(x_0, u_0)\delta u. \tag{3.11}$$

Where (x_0, u_0) is the operating point of the studied model. Therefore the linearization can be realized around this operating point. Then the vector representation of input and output is as follows:

$$\delta x = [\delta I_d, \delta I_q, \delta V_{bus,d}, \delta V_{bus,q}, \delta I_{dc}, \delta V_{dc}, \delta I_s, \delta \omega_r]^T \tag{3.12}$$

$$\delta u = [\delta V_o]^T. \tag{3.13}$$

Now the A(x_0, u_0) and B(x_0, u_0) matrices can be constructed around the equilibrium point. Since there are eight states and one input the size of matrix A is 8 x 8 and the size of matrix B is 8 x 1. State-space form after linearization is represented in equation (3.14).

$$\dot{x} = \begin{bmatrix} \frac{-R_{eq}}{L_{eq}} & \omega & \frac{-1}{L_{eq}} & 0 & 0 & \sqrt{\frac{3}{2}}\frac{1}{K_d} & 0 & 0 \\ \frac{-R_{eq}}{L_{eq}} & -\omega & 0 & \frac{-1}{L_{eq}} & 0 & \sqrt{\frac{3}{2}}\frac{1}{K_q} & 0 & 0 \\ \frac{1}{C_{eq}} & 0 & 0 & \omega & -\frac{3\sqrt{2}}{\pi} & 0 & 0 & 0 \\ 0 & \frac{1}{C_{eq}} & -\omega & 0 & 0 & 0 & 0 & 0 \\ 0 & 0 & \frac{3\sqrt{2}}{\pi L_F} & 0 & \frac{R_F}{L_F} & \frac{-1}{L_F} & 0 & 0 \\ 0 & 0 & 0 & 0 & 0 & \frac{1}{C_F} & 0 & \frac{-P_{cpl}}{C_F V_{out}} \\ 0 & 0 & 0 & 0 & 0 & \frac{1}{L_{sm}} & \frac{-R_{sm}}{L_{sm}} & \frac{-PF_m}{2L_{sm}} \\ 0 & 0 & 0 & 0 & \frac{K_T}{J_m} & 0 & 0 & 0 \end{bmatrix} x + \begin{bmatrix} 0 \\ 0 \\ 0 \\ 0 \\ 0 \\ 0 \\ 0 \\ 1 \end{bmatrix} u \tag{3.14}$$

Where dq transformation coefficients K_d and K_q are as follows:

$$K_d = [\cos(\theta)+\cos(\theta-2\pi/3)+\cos(\theta+2\pi/3)] \tag{3.15}$$

$$K_q = [\sin(\theta)+\sin(\theta-2\pi/3)+\sin(\theta+2\pi/3)]. \tag{3.16}$$

Besides that, the input-output relation around this operating point can be expressed in equation (3.15):

$$y = [0 \quad 0 \quad 0 \quad 0 \quad 0 \quad 1 \quad 0 \quad 0]x + [0]\, u\,. \tag{3.17}$$

On the other hand, since the rectifier model is transformer-like model it is necessary to convert the expression into their per unit counterparts. Appendix-A explains how per unit conversion is implemented on the state space expressions. Base voltage and base power are taken as V_{bac}= 230 V, S_{bac}= 50 kW for the AC side of rectifier. Furthermore, V_{bdc}= 500 V, and S_{bdc}= 25 kW for the DC side of the rectifier. Therefore the base current for AC side is I_{bac}= S_{bac}/V_{bac}=1000/230=4.35 A. Similarly, the base current for DC side is I_{bdc}= S_{bdc}/V_{bdc}=2000/500=40 A. After per unit conversion and substituting the values into the matrix according to the table in Appendix B the problem is ready to be solved. Now we have A, B, C, and D matrices of the plant. Therefore the constraints for the LQR problem is provided by the help of those matrices. But it is essential to check whether the plant is controllable or not according to A and B matrices. The following matrix form will help to check controllability of the power system:

$$\mathbb{C} = [B \quad AB \quad A^2B \quad \cdots \quad A^{n-1}B]. \tag{3.18}$$

Where A is n x n matrix and in this study ***n*** is equal to 8. The rank of controllability matrix must be equal to n to assure the system is controllable. After evaluating the controllability matrix it is obvious that the power is controllable. In chapter 4 the simulation and stability issue will be examined.

3.3 LINEAR QUADRATIC REGULATOR (LQR)

Since the converters and motor drives are dependent on time and they have nonlinear destabilizing characteristics an appropriate control method is necessary to avoid instability. However classical control methods such as PI ([2]. **Error! Reference source not found.**, [5]. [6]. [7], [12]) or PID [13], [14]. [15]) have stability limitations because of the operation range. On the other hand, optimal control methods may expand these limitations if the parameters are properly tuned. As one the optimal control methods linear quadratic regulators is able to solve continuous state-space optimal control problem properly but it needs the control problem to be linear. Therefore to solve the problem obtaining the differential equations, linearization of the system, and generation of state-space matrices must be done respectively. Figure 16. shows a general linear quadratic regulator control block diagram.

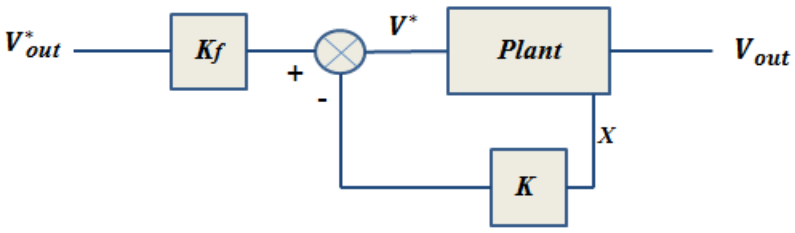

Figure 16. Linear Quadratic Regulator Model

In Figure 16. the 'y' represents **output**, 'x' represents **states**, 'r' represents **reference** and 'u' represent the **input** or **control signal**. 'K' block stands for Kalman gain and 'K_f' is feed-forward gain. Next chapter will explain how Kalman gain and feed-forward gain are calculated.

4.0 SIMULATIONS AND STABILITY ANALYSIS

4.1 STABILITY CONDITION

When we check the eigenvalues of the state matrix by using MATLAB the following results are obtained:

Table 1. Eigenvalues of matrix A (P_{cpl}=25 kW)

22.88	6.73+j16.33	6.73-j16.33	-4.34+j18.22
-4.34-j18.22	-3.17+j2.28	-3.17-j2.28	-17.90

Table 2. Eigenvalues of matrix A (P_{cpl}=50 kW)

25.81	8.73+j19.51	8.73-j19.51	-6.18+j22.13
-6.18-j22.13	-4.71+j3.79	-4.71-j3.79	-20.88

As seen from the table all eigenvalues are in the right-half-plane except three of them. In Figure 17. and Figure 18. the step response of the power system without controller is shown. These figure are plotted when CPL power is equal to 25 kW and 50 kW.

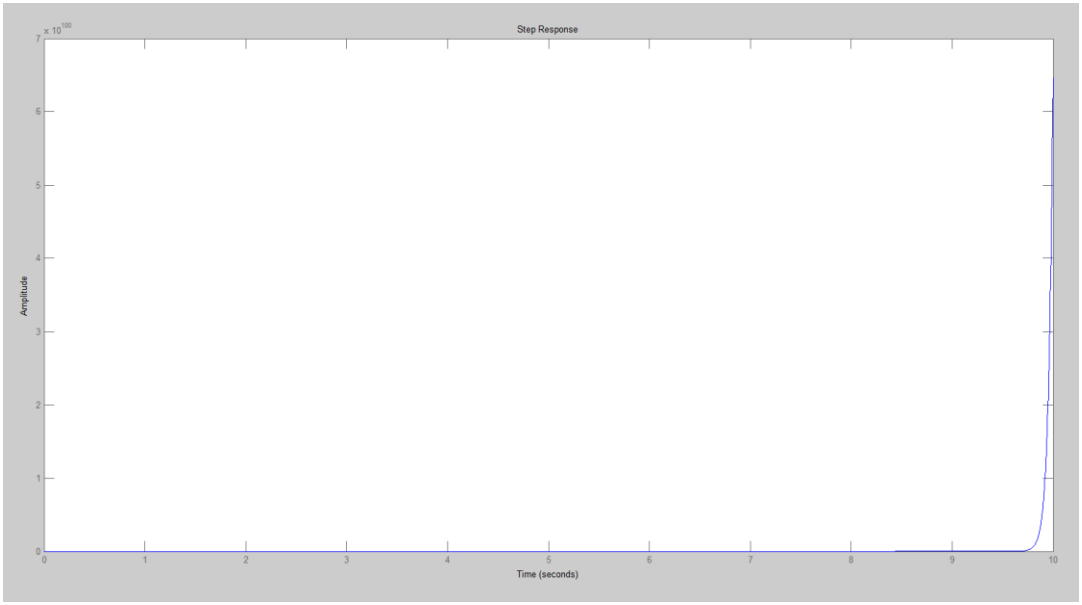

Figure 17. Step response of the power system (P_{cpl}=25 kW)

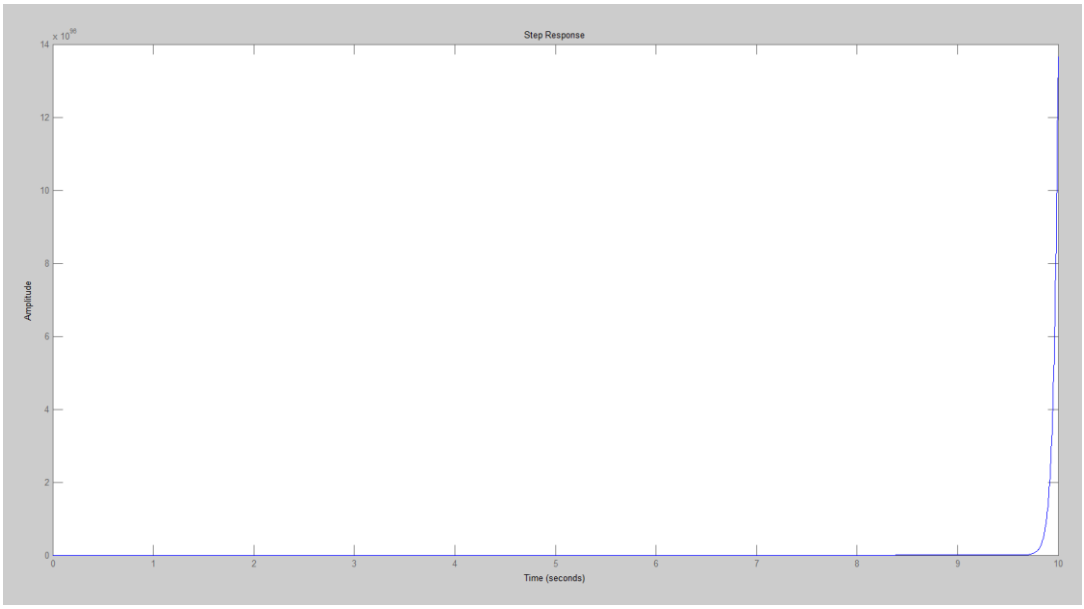

Figure 18. Step response of the power system (P_{cpl}=50 kW)

As seen from the figure the step response of the system doesn't converge to any point. It means that it needs to be controlled. Therefore to make the power system stable a linear quadratic

regulator with proper weight matrices will be used. An algorithm has been come up to realize the MATLAB code. The following figure summarizes the algorithm for simulation:

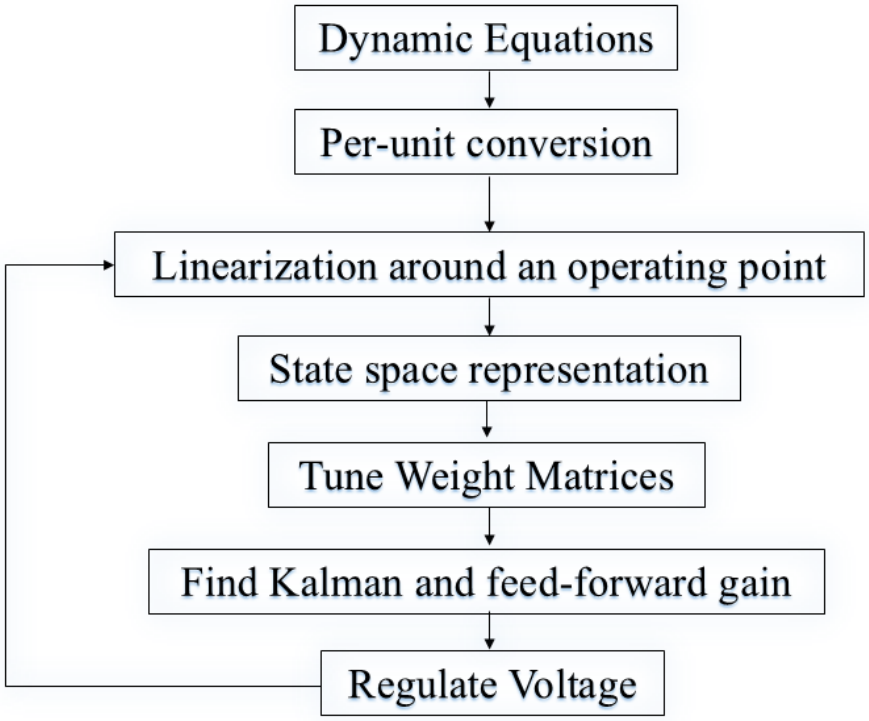

Figure 19. Flow chart of the algorithm for the simulations

As shown in the flow chart, at the beginning the differential equations of the model or power system need to be obtained. Then on both AC and DC side per-unit conversion should be realized. To be able to use LQR as a controller linearization around an operating point is necessary. After that the states can be written in the matrix form. State-feedback and feed-forward gains can be calculated by choosing the appropriate weight matrices. Finally, the voltage can be regulated.

Stabilization of the system under different power ratings requires the selection of correct weight matrices (***Q*** and ***R***). In the next section the selection of the weight matrices and the step responses for different weight matrices will be examined.

4.2 WEIGHT MATRIX SELECTION

As stated before the LQR controller generates the state feedback (***K***) gain. Additionally, since the input and output of the studied model doesn't have an effect on the output simultaneously the performance index can be rewritten is as follows:

$$J(t) = \int_0^\infty (x^T Q x + u^T R u) dt. \tag{4.1}$$

While generating the parameters of the gain it minimizes the error in equation (4.1). MATLAB has a function which is called '**lqr**' to generate K matrix of the LQR controller. However it is necessary to tune ***Q***, ***R***, and ***N*** matrices. Since the input and the states affect the performance index respectively the matrix ***N*** is zero matrix. R matrix is 1x1 matrix and it is chosen as 1 in this study. On the other hand, the ***Q*** matrix is 8 x 8 matrix which is necessary to be tuned appropriately. First, matrix ***Q*** is chosen as identity matrix $\mathbf{I_8}$. However it didn't give the expected results. These are the several ***Q*** matrices which are selected to compare different step responses of the system:

$$Q_1 = I_8 \tag{4.2}$$

$$Q_2 = 100 * I_8 \tag{4.3}$$

$$Q_3 = \begin{bmatrix} 100 & 0 & 0 & 0 & 0 & 0 & 0 & 0 \\ 0 & 100 & 0 & 0 & 0 & 0 & 0 & 0 \\ 0 & 0 & 1 & 0 & 0 & 0 & 0 & 0 \\ 0 & 0 & 0 & 1 & 0 & 0 & 0 & 0 \\ 0 & 0 & 0 & 0 & 100 & 0 & 0 & 0 \\ 0 & 0 & 0 & 0 & 0 & 100 & 0 & 0 \\ 0 & 0 & 0 & 0 & 0 & 0 & 1 & 0 \\ 0 & 0 & 0 & 0 & 0 & 0 & 0 & 1 \end{bmatrix} \tag{4.4}$$

$$Q_4 = \begin{bmatrix} 1 & 0 & 0 & 0 & 0 & 0 & 0 & 0 \\ 0 & 100 & 0 & 0 & 0 & 0 & 0 & 0 \\ 0 & 0 & 1 & 0 & 0 & 0 & 0 & 0 \\ 0 & 0 & 0 & 100 & 0 & 0 & 0 & 0 \\ 0 & 0 & 0 & 0 & 1 & 0 & 0 & 0 \\ 0 & 0 & 0 & 0 & 0 & 100 & 0 & 0 \\ 0 & 0 & 0 & 0 & 0 & 0 & 1 & 0 \\ 0 & 0 & 0 & 0 & 0 & 0 & 0 & 100 \end{bmatrix}. \tag{4.5}$$

'lqr' function on MATLAB always returns a stabilizing gain matrix provided that the state matrix ***A*** is controllable via the input matrix ***B***. This function doesn't care about the output and output matrices ***C*** and ***D***. It only makes the closed loop plant stable by using the state feedback gain ***K***. The following figure shows the step responses for different weight matrices (Q_1 through Q_4):

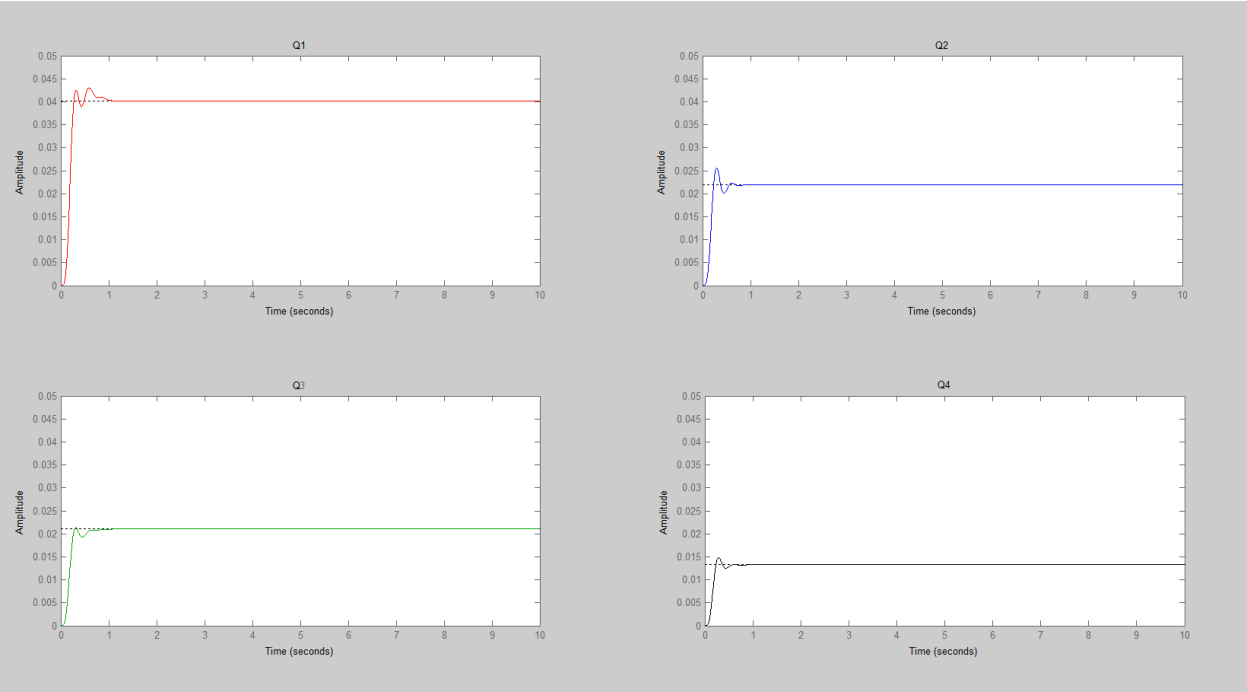

Figure 20. Step responses for weight matrices $Q_{1,2,3,4}$

The state feedback gain matrix ***K*** provides better attributes at the plant when it is compared to conventional controller gains. Furthermore, the magnitude of the weighting parameter is inversely proportional to the weighted signal. For instance increasing the weighting parameter will minimize the weighted signal. When the step responses of the system with Q_1 and Q_2 weight matrices is compared the increment on the Q matrix causes the reduction of the weighted signal. Therefore to minimize the effect of some states it is necessary to increase the weighting parameter of those states. In other words, **"one balance the rate of convergence of the trajectories with the cost of the control"**. [17] By comparing the step responses the weight matrix is selected to get the best result so that state feedback gain can be obtained. The chosen weight matrix is as follows:

$$Q = \begin{bmatrix} 1 & 0 & 0 & 0 & 0 & 0 & 0 & 0 \\ 0 & 100 & 0 & 0 & 0 & 0 & 0 & 0 \\ 0 & 0 & 1 & 0 & 0 & 0 & 0 & 0 \\ 0 & 0 & 0 & 1 & 0 & 0 & 0 & 0 \\ 0 & 0 & 0 & 0 & 1 & 0 & 0 & 0 \\ 0 & 0 & 0 & 0 & 0 & 0.1 & 0 & 0 \\ 0 & 0 & 0 & 0 & 0 & 0 & 1 & 0 \\ 0 & 0 & 0 & 0 & 0 & 0 & 0 & 100 \end{bmatrix}. \quad (4.6)$$

Figure 21. shows the step response of the overall system without and with feed-forward gain K_{ff}:

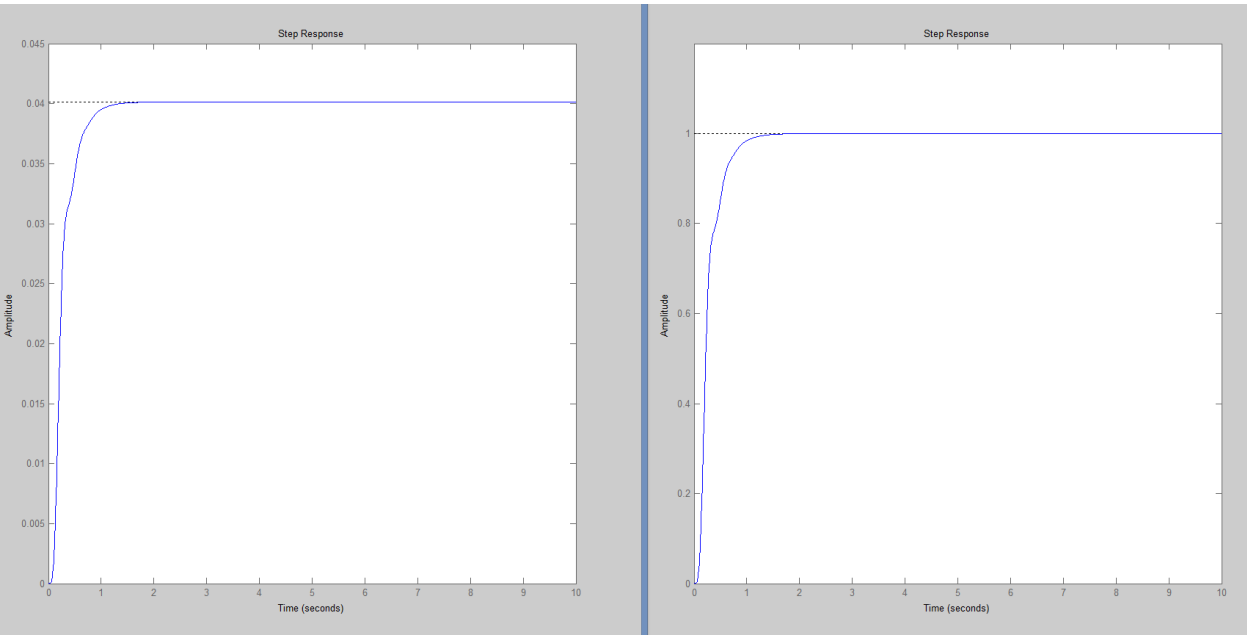

Figure 21. Step response without K_{ff} (Left) and with K_{ff} (Right)

As shown in the figure, without feed-forward gain the system is not able to converge DC unit gain. However, by the help of that gain unit gain can be obtained. Feed forward gain, K_{ff}, is calculated as 28.95 for three-phase system. It provides very accurate results. Moreover, settling of the closed loop system is faster than conventional control methods. Besides that the overshoot can be eliminated by choosing the correct weight matrix. It can said that the control algorithm has faster settling and less overshoot characteristics than conventional control methods. Moreover, if the load

power is increased it will cause more oscillation. In this case the plant might not converge to any point which makes the system unstable. [20] On the other hand, several literatures ([15], [17] and [19]) have reported the robustness performance of LQR controller, with the cost of hardware and software complexity. To check the system stability it might be useful to look at the root locus plot of the dynamic system. Figure 22. represents the root locus plot of the system when the CPL power is equal to 25 kW.

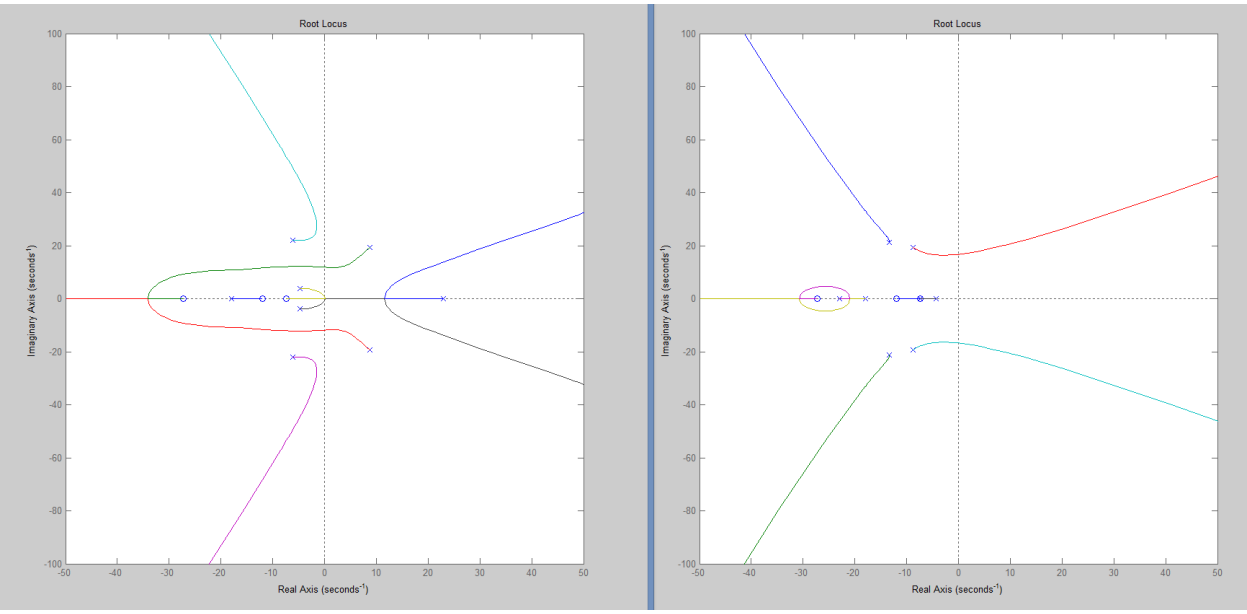

Figure 22. Root locus of the dynamic system without (Left) and with controller (Right)

It can be seen from the figure that three roots of the dynamic system are located in the right-half plane. However using LQR and choosing the weighting matrix of the controller properly shifts all the poles to the negative-half plane. Therefore the system is stabilized. On the other hand, root locus figure is also plotted when CPL power is equal to 50 kW. Figure 23. shows the root locus plot of the dynamic system when constant power is increased to 50 kW.

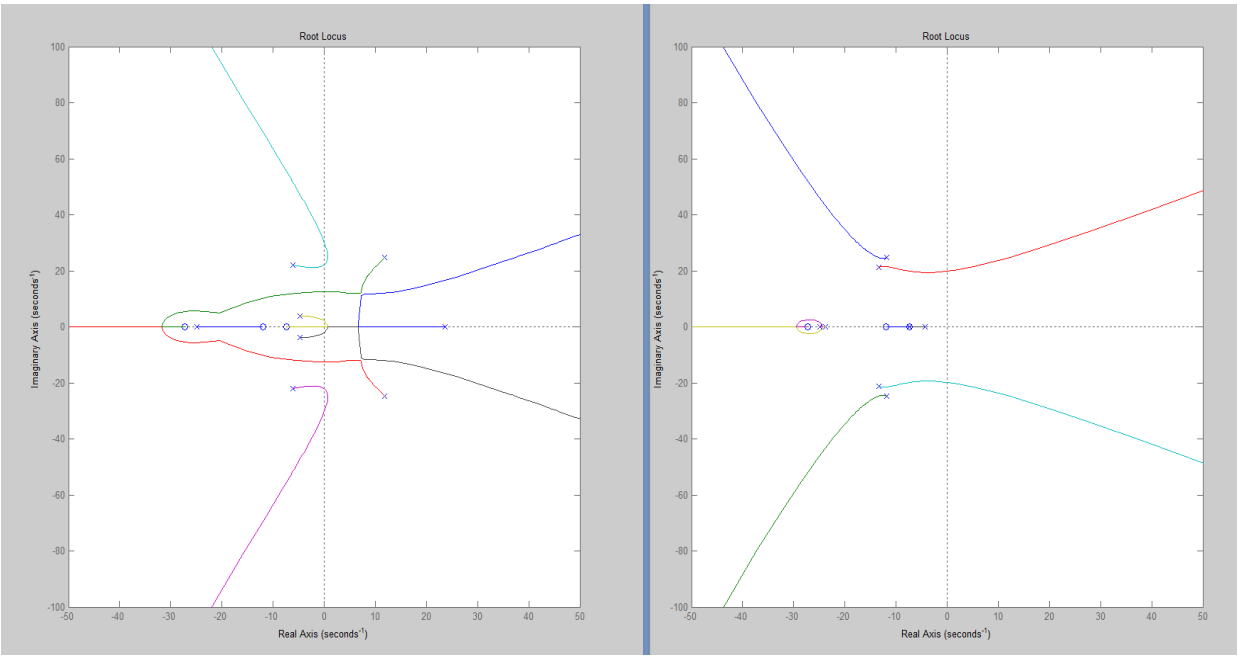

Figure 23. Root locus plot of dynamic system without (Left) and with controller (Right)

Using linear quadratic regulator is able to replace closed loop poles of a linear control system. Moreover, the poles can be moved to the specified places on the plane by choosing appropriate weight matrices. Although estimation of robustness and dynamic error can be done in a linear control system, choosing the optimum weight matrices is very difficult for vehicle systems since the vehicle power systems have nonlinear characteristics. [21] Because of that the linearization of the system and some assumptions is very crucial to be able to obtain results.

State feedback and feed-forward gain is multiplied by the state variables in this closed loop system. Furthermore, difference between reference speed and the feedback signal and is applied to a comparator circuit. Then this circuit generates switch pulses to turn on and off the gates of diodes in the rectifier. Unfortunately it might cause too much power consumption. Even though this control algorithm provides robust and better solutions when it is compared to conventional control methods its efficiency might be lower because of more power consumption. [22]

Now let's look at the one-phase system since some aircrafts and more electric vehicles might use one-phase generator. As mentioned earlier state space representation of one-phase system was obtained in the literature [1]. The first harmonic approximation is used since most of the small perturbation occurs at the first harmonic. To be able to use that dynamic model it is needed to do per-unit conversion. In Appendix-A dynamic equations are rewritten according to per-unit conversion. In this method instead of referencing the rotor speed load voltage is used as an input. However, making changes in the CPL caused the tightly regulated output to be sacrificed. [23] While using LQR in the one-phase power distribution system the weight matrices are specified. ***R*** is again taken as ***I***, identity matrix, and ***Q*** matrix is calculated by using ***C***'***C*** formula. Then step response and root-locus graphs of the dynamic model are plotted on MATLAB. Figure 24. shows the step response of the system with and without controller.

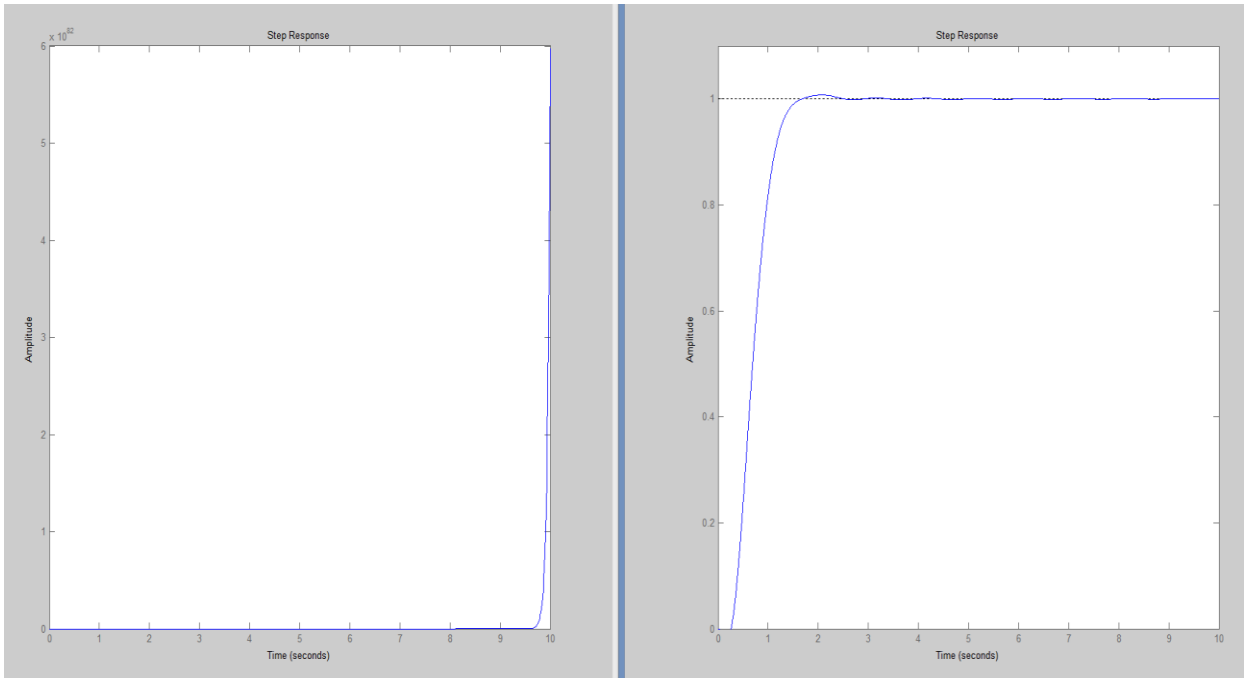

Figure 24. Step response of the model without (left) and with controller (right)

As seen from this figure again step response without controller doesn't converge any value. Instead it goes to very huge value like $6*10^{23}$. In contrast to that, it reaches steady state when linear quadratic regulator is used in that system. Its' settling time is very fast and there is almost no overshoot in the voltage just like in three-phase system. Additionally, looking at root-locus plots of the dynamic system might help us to understand the stability characteristics of the system. Figure 25. represents the root-locus plot of the power system with and without controller.

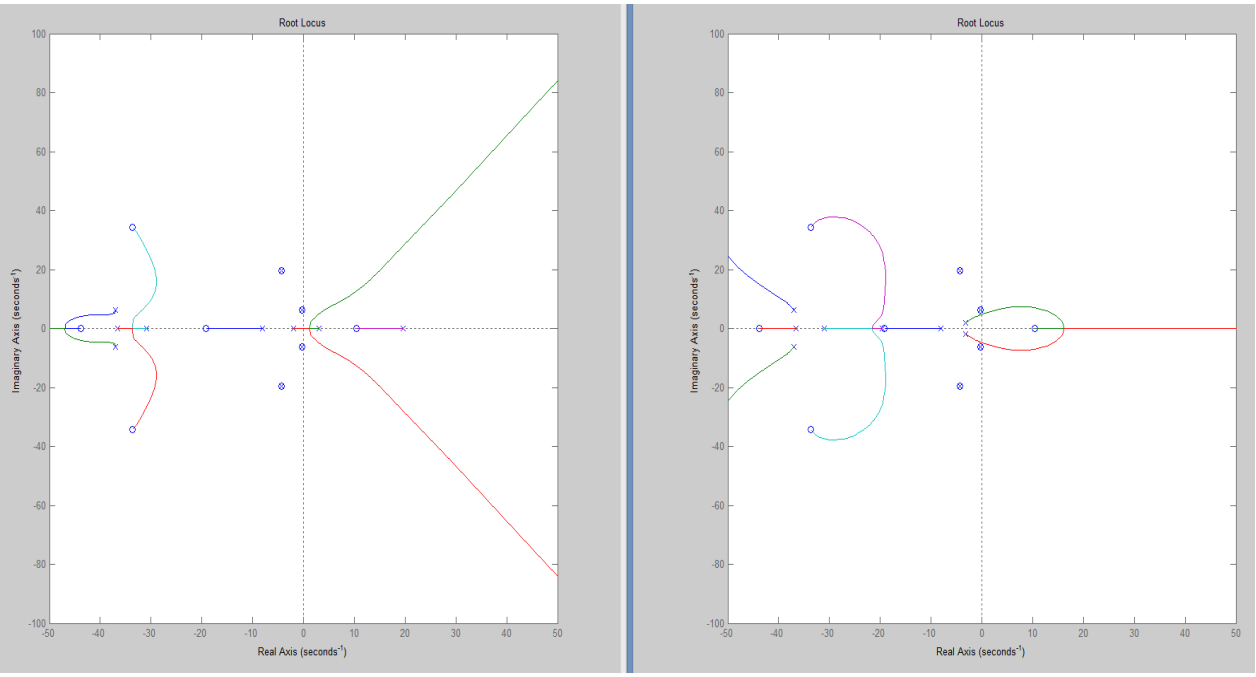

Figure 25. Root-locus graphs of the system without (left) and with LQR (right)

In the left figure it can be seen that there are 2 poles on the right-half plane and the other 10 poles are on the left-half plane. Therefore these 2 poles located on the positive x-axis makes the system unstable. By choosing correct weight matrices (***Q***, and ***R***) and using linear quadratic regulator we are able to move all the poles to the left-half plane so that the system can be stabilized and is able to reach steady state.

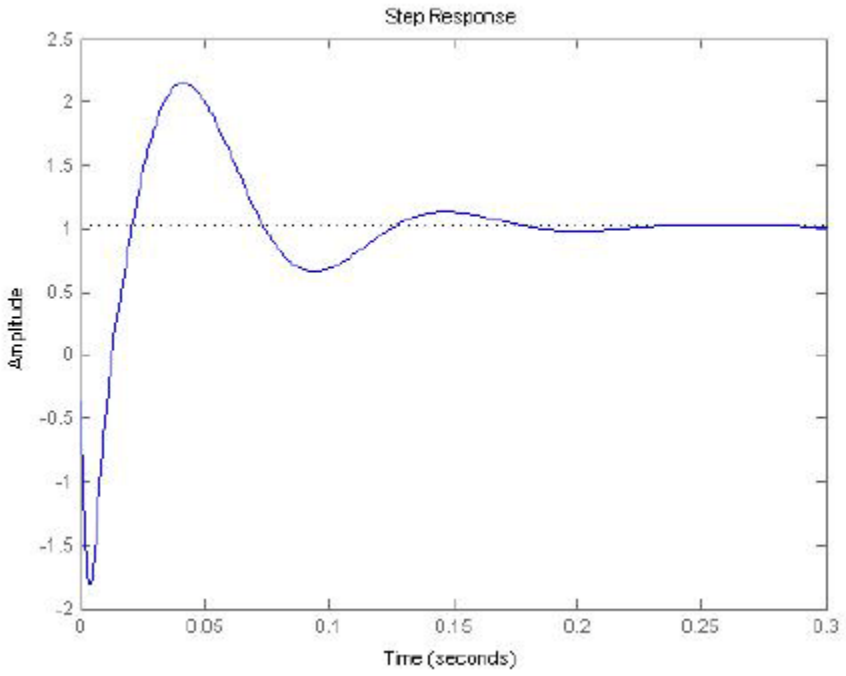

Figure 26. The step response with a conventional controller when CPL is equal to 50 kW (Adapted from [25])

Figure 26. depicts the step response when the CPL is equal to 50 kW. In this study [25] cascaded two PI controllers are used to regulate both voltage and current. As seen from the graph settling is very slow and overshoot is too high in this case when it is compared to the result with LQR. If the weight matrices are chosen in a correct way it is possible to reduce the overshooting and settling time to the desired value.

5.0 CONCLUSION

In this study constant power load issue in more electric aircraft power systems and solution to this instability effect is explained. Negative impedance instability characteristics of constant power loads are discussed. Besides that, the plant has a motor drive system so the electromechanical actuator behaves as a constant power load. As an electric motor PMSM used and the advantages and disadvantages of permanent magnet synchronous machine (PMSM) over induction machine (IM) are explained.

To represent the model in matrix form, the differential equations of the model are obtained. Per-unit conversion is realized after simplification of the power system. The states are represented in matrix form. An optimal control problem to solve this problem is defined by using the state-space representation of the model. Construction of the optimal control problem is done with its states, input performance index, and constraints. Linear quadratic regulator is applied to the plant. LQR needs the information of all states. Therefore it may require sensors to measure the data from every state. In contrast to that, state estimators can be used to get the information from all the states, especially when the state is not available in real implementation. For instance, the current and voltage information in rotating frame (dq0 transformation) is not accessible. Therefore the usage of state estimators would be very beneficial in that case.

To be able to solve the optimal control problem Riccati equation needs to be written. The solution to Riccati equation is used to find the state feedback gain. The solution to the Riccati equation and Kalman gain, i.e. state feedback gain, are found by using MATLAB function ***'lqr'***. Moreover, figures for step responses and root-locus curves are plotted by using the same software.

LQR controlled plant is settled to output voltage when it is loaded with constant power load. Similarly, state feedback controlled power system tracks the desired output in a good manner. Furthermore how LQR in the closed loop system enhance the stability of MEA EPS is discussed. Additionally, the efficiency and robustness of the state feedback control method is stated.

In conclusion, the motor drive systems and power electronic converters behave as constant power load. Constant power load has negative incremental impedance characteristics. This issue narrows the stability margin of the power system. To be able to solve the instability problem it is necessary to use a controller to regulate the voltage.

Optimal controller is used in this study to regulate the voltage. Besides that, an algorithm for the simulations is constructed. This control algorithm works well for different power ratings and has important advantages over conventional control methods. It reduces the overshooting and the settling time of the system in a huge amount.

APPENDIX A

PER UNIT CONVERSION

While analyzing power systems, it might be useful to convert the system to a per unit system to normalize system variables. A well-chosen per unit system can minimize computational effort. A quantity in per unit is defined as the ratio of that quantity to a selected base quantity of the same nature. Voltage and power are selected as base quantities for per unit conversion. Because for each voltage level in the studied system, the rated voltage of the equipment is known. Besides that, even though the power load changes, the voltage doesn't deviate too much from the rated value. In addition to that, the range of power which flows in a section of the system is quadratically related with the voltage. [24] The per unit expressions for voltage, power, current and impedance can be shown in the following form:

$$V_{base} = V_{\phi-\phi} \tag{A.1}$$

$$S_{base} = S_{3\phi} \tag{A.2}$$

$$I_{base} = \frac{S_{base}}{\sqrt{3}V_{base}} \tag{A.3}$$

$$Z_{base} = \frac{{V_{base}}^2}{S_{base}} \tag{A.4}$$

The equations (2.23-26) can be rearranged according to per unit conversion. New equations can be written as follows:

$$\frac{v_{ac}}{V_{b1}} = \frac{R_{eq}.i_1}{V_{b1}} + \frac{L_{eq}}{V_{b1}}.\frac{di_1}{dt} + \frac{v_{in}}{V_{b1}} \tag{A.5}$$

$$\frac{V_{b1}C_{eq}}{S_{b1}}.\frac{dv_{in}}{dt} + \frac{V_{b1}i_{in}}{S_{b1}} = \frac{V_{b1}i_1}{S_{b1}} \tag{A.6}$$

$$\frac{v_{out}}{V_{b2}} = \frac{R_F.i_{out}}{V_{b2}} + \frac{L_F}{V_{b2}}.\frac{di_{out}}{dt} + \frac{v_o}{V_{b2}} \tag{A.7}$$

$$\frac{V_{b2}C_F}{S_{b2}}.\frac{dv_o}{dt} + \frac{V_{b2}}{S_{b2}}\frac{P_{cpl}}{v_o} + \frac{V_{b2}}{S_{b2}}\frac{v_o}{R} = \frac{V_{b2}i_{out}}{S_{b2}} \tag{A.8}$$

Normally state space expression of the model in Figure 13. was:

$$\dot{X} = \begin{bmatrix}
\frac{-R_{eq}}{L_{eq}} & \frac{-1}{L_{eq}} & 0 & 0 & 0 & 0 & 0 & 0 & 0 & 0 & 0 & 0 \\
\frac{1}{C_{eq}} & 0 & 0 & 0 & 0 & 0 & 0 & 0 & 0 & \frac{4}{\pi C_{eq}} & 0 & 0 \\
0 & 0 & \frac{-R_F}{L_F} & \frac{-1}{L_F} & 0 & 0 & 0 & \frac{-4}{\pi L_F} & 0 & 0 & 0 & 0 \\
0 & 0 & \frac{1}{C_F} & \frac{-1}{RC_F} + \frac{P}{C_F {V_o}^2} & 0 & 0 & 0 & 0 & 0 & 0 & 0 & 0 \\
0 & 0 & 0 & 0 & \frac{-R_{eq}}{L_{eq}} & \omega & \frac{-1}{L_{eq}} & 0 & 0 & 0 & 0 & 0 \\
0 & 0 & 0 & 0 & -\omega & \frac{-R_{eq}}{L_{eq}} & 0 & \frac{-1}{L_{eq}} & 0 & 0 & 0 & 0 \\
0 & 0 & 0 & 0 & \frac{1}{C_{eq}} & 0 & 0 & \omega & 0 & 0 & 0 & 0 \\
0 & 0 & \frac{2}{\pi C_{eq}} & 0 & 0 & \frac{1}{C_{eq}} & -\omega & 0 & 0 & 0 & 0 & 0 \\
0 & 0 & 0 & 0 & 0 & 0 & 0 & 0 & \frac{-R_F}{L_F} & \omega & \frac{-1}{L_F} & 0 \\
0 & \frac{-2}{\pi L_F} & 0 & 0 & 0 & 0 & 0 & 0 & -\omega & \frac{-R_F}{L_F} & 0 & \frac{-1}{L_F} \\
0 & 0 & 0 & \frac{-2Pcos(\theta)}{C_F {V_o}^2} & 0 & 0 & 0 & 0 & \frac{1}{C_F} & 0 & \frac{-1}{RC_F} + \frac{P}{C_F {V_o}^2} & \omega \\
0 & 0 & 0 & \frac{-2Psin(\theta)}{C_F {V_o}^2} & 0 & 0 & 0 & 0 & 0 & \frac{1}{C_F} & -\omega & \frac{-1}{RC_F} + \frac{P}{C_F {V_o}^2}
\end{bmatrix} X + \begin{bmatrix} 0 \\ 0 \\ 0 \\ 0 \\ 0 \\ \frac{-1}{2L_{eq}} \\ 0 \\ 0 \\ 0 \\ 0 \\ 0 \\ 0 \end{bmatrix} u \tag{A.9}$$

After per unit conversion state space representation of one-phase power system becomes:

$$\dot{X} = \begin{bmatrix}
\frac{-R_{eq}}{L_{eq} * V_{b1}} & \frac{-1}{L_{eq} * V_{b1}} & 0 & 0 & 0 & 0 & 0 & 0 & 0 & 0 & 0 & 0 \\
\frac{V_{b1}}{C_{eq} * S_{b1}} & 0 & 0 & 0 & 0 & 0 & 0 & 0 & 0 & \frac{4 * V_{b1}}{\pi C_{eq} * S_{b1}} & 0 & 0 \\
0 & 0 & \frac{-R_F}{L_F * V_{b2}} & \frac{-1}{L_F * V_{b2}} & 0 & 0 & 0 & \frac{-4}{\pi L_F * V_{b2}} & 0 & 0 & 0 & 0 \\
0 & 0 & \frac{V_{b2}}{C_F * S_{b2}} & \frac{-V_{b2}}{R * C_F * S_{b2}} + \frac{P_{cpl} * V_{b2}}{C_F {V_o}^2 * S_{b2}} & 0 & 0 & 0 & 0 & 0 & 0 & 0 & 0 \\
0 & 0 & 0 & 0 & \frac{-R_{eq}}{L_{eq} * V_{b1}} & \frac{\omega}{V_{b1}} & \frac{-1}{L_{eq} * V_{b1}} & 0 & 0 & 0 & 0 & 0 \\
0 & 0 & 0 & 0 & \frac{-\omega}{V_{b1}} & \frac{-R_{eq}}{L_{eq} * V_{b1}} & 0 & \frac{-1}{L_{eq} * V_{b1}} & 0 & 0 & 0 & 0 \\
0 & 0 & 0 & 0 & \frac{V_{b1}}{C_{eq} * S_{b1}} & 0 & 0 & \frac{V_{b1} * \omega}{S_{b1}} & 0 & 0 & 0 & 0 \\
0 & 0 & \frac{2 * V_{b1}}{\pi C_{eq} * S_{b1}} & 0 & 0 & \frac{V_{b1}}{C_{eq} * S_{b1}} & \frac{-V_{b1} * \omega}{S_{b1}} & 0 & 0 & 0 & 0 & 0 \\
0 & 0 & 0 & 0 & 0 & 0 & 0 & 0 & \frac{-R_F}{L_F * V_{b2}} & \frac{\omega}{V_{b2}} & \frac{-1}{L_F V_{b2}} & 0 \\
0 & \frac{-2}{\pi L_F * V_{b2}} & 0 & 0 & 0 & 0 & 0 & 0 & \frac{-\omega}{V_{b2}} & \frac{-R_F}{L_F * V_{b2}} & 0 & \frac{-1}{L_F * V_{b2}} \\
0 & 0 & 0 & \frac{-2P_{cpl} cos(\theta) * V_{b2}}{C_F {V_o}^2 * S_{b2}} & 0 & 0 & 0 & 0 & \frac{V_{b2}}{C_F * S_{b2}} & 0 & \frac{-V_{b2}}{R * C_F * S_{b2}} + \frac{P_{cpl} * V_{b2}}{C_F {V_o}^2 * S_{b2}} & \frac{\omega * V_{b2}}{S_{b2}} \\
0 & 0 & 0 & \frac{-2P_{cpl} sin(\theta) * V_{b2}}{C_F {V_o}^2 * S_{b2}} & 0 & 0 & 0 & 0 & 0 & \frac{V_{b2}}{C_F * S_{b2}} & \frac{-\omega * V_{b2}}{S_{b2}} & \frac{-V_{b2}}{R * C_F * S_{b2}} + \frac{P_{cpl} * V_{b2}}{C_F {V_o}^2 * S_{b2}}
\end{bmatrix} X \quad \text{(A.10)}$$

$$+ \begin{bmatrix} 0 \\ 0 \\ 0 \\ 0 \\ 0 \\ \frac{-1}{2L_{eq} * V_{b1}} \\ 0 \\ 0 \\ 0 \\ 0 \\ 0 \\ 0 \end{bmatrix} u$$

APPENDIX B

SYSTEM PARAMETERS

Table 3. Parameters for the simulations

Parameters	**Value**
Generator Voltage (rms per phase): V_{ac}	*230 V*
Frequency: f	*50 Hz*
Angular speed: ω	*314 rps*
Equivalent input resistance: R_{eq}	*0.05 Ω*
Equivalent input inductance: L_{eq}	*25 μH*
Equivalent input capacitance: C_{eq}	*2 nF*
Filter resistance: R_F	*0.5 Ω*
Filter inductance: L_F	*5 mH*
Filter capacitance: C_F	*1 mF*
Inductor of the synchronous machine: L_{sm}	*0.6 mH*
Resistor of the synchronous machine: R_{sm}	*0.75 Ω*
Number of poles in the synchronous machine : P	*20*
EMF constant of the synchronous machine : F_m	*0.125 Wb*
Inertia of the synchronous machine : J_m	*4000 kgm^2*
Torque constant of the synchronous machine : K_T	*1.875 Nm/Amp*
Rated torque of the load: T_l	*25 Nm*

BIBLIOGRAPHY

[1]. Emadi, A.; Ehsani, M.; Miller, J.M. “Vehicular Electric Power Systems: Land, Sea, Air and Space Vehicles” CRC Press, 2003.

[2]. Emadi, A.; Fahimi, A.; and Ehsani, M. “On the Concept of Negative Impedance Instability in the More Electric Aircraft Power Systems with Constant Power Loads, Soc. Automotive Eng. J., pp.689-699, 1999

[3]. Areerak, K. “Modelling and stability analysis of aircraft power systems” Diss, University of Nottingham, 2009

[4]. Reed, G.F.; Grainger, B.M.; Sparacino, A.R.; Mao, Z.H. "Ship to Grid: Medium Voltage DC Concepts in Theory and Practice" IEEE Power and Energy Magazine, Vol. 10, No. 6, pp. 70-79, Nov/Dec.2012.

[5]. Gruzs, T., and Hall, J. "AC, DC or Hybrid Power Solutions for Today's Telecommunications Facilities," Telecommunications Energy Conference. INTELEC 2000. Twenty-second International, pp. 361-368, 2000

[6]. Monti, A., Boroyevich, D., Cartes, D., Dougal, R., Ginn, H., Monnat, G., Pekarek, S., Ponci, F., Santi, E., Sudho, S., Schulz, N., Shutt, W., and Wang, F. "Ship Power System Control: A Technology Assessment," Electric Ship Technologies Symposium, pp. 292-297, 2005.

[7]. Monti, A., Liu, R., Deshmukh, A., Ponci, F., and Dougal, R. "Towards a New Fully-Flexible Control Approach for Distributed Power Electronics Building Block Systems", Proc. 34th IEEE IECON, pp.2955 -2961 2008

[8]. Louganski, K.P. "Modeling and Analysis of a DC Power Distribution System in 21st Century Airlifters", Diss, Virginia Polytechnic Institute and State University, 1999

[9]. Emadi, A. "Modeling of power electronic loads in AC distribution systems using the generalized state-space averaging method." *Industrial Electronics, IEEE Transactions on* 51.5 (2004): 992-1000.

[10]. Coulomb, J-M. “Stability Analysis and Optimal Control Design for AC-DC Power System with Constant Power Load” Diss. University of Pittsburgh, 2012.

[11]. Mohan, N., Underland, T.M., and Robbins, W.P. “Power Electronics: Converters, Applications, and Design” John Wiley & son, USA, 2003, pp. 105-110.

[12]. Areerak, K-N., Bozhko, S.V., de Lillo, L., Asher, G.M., Thomas, D.W.P., Watson, A., Wu, T. “The Stability Analysis of AC-DC Systems Including Actuator Dynamics for Aircraft Power Systems,” In Proceedings of the 13th European Conference on Power Electronics and Applications, (EPE 2009), Barcelona, Spain, Sept. pp.8-10,2009

[13]. Tabatabaei, N.M., and Shokouhian M.R. "Designing Power System Stabilizer with PID Controller." *International Journal on Technical and Physical Problems of Engineering (IJTPE)* 3 (2010): 1-7.

[14]. Theja, B.S., et al. "Design of PID Controller Based Power System Stabilizer Using Modified Philip-Heffron's Model: an Artificial Bee Colony Approach." Swarm Intelligence (SIS), 2013 IEEE Symposium on. IEEE, 2013.

[15]. Yousef, A. M., and El-Sherbiny, M. K. "Improvement of Synchronizing and Damping Torque Coefficients Based LQR Power System Stabilizer." *Electrical, Electronic and Computer Engineering, 2004. ICEEC'04. 2004 International Conference on*. IEEE, 2004.

[16]. "Linear-Quadratic Regulator (LQR) design" Web document. Retrieved from http://www.mathworks.com/help/control/ref/lqr.html on 05/12/2014

[17]. Verde, C., Rojas A.J. L., and Fuerte-Esquivel, C.R "Improving Stability Margin in Electric Power Systems by Linear Quadratic Regulator and Disturbance Model." *Electric Power Components and Systems* 41.14 (2013): 1415-1431.

[18]. Mihailovic, Z. “Modeling and Control Design of VSI-fed PMSM Drive Systems with Active Load*”* Diss. Virginia Polytechnic Institute and State University, 1998.

[19]. Verde, C., and Frank, P. M., “Sensitivity Reduction of the Linear Quadratic Regulator by Matrix Modification,” Int. J. Control, Vol. 48, pp. 211–223, 1988.

[20]. Yousef, A. M., "Power System Controller Design Based on Robust H_2 theory" Journal of Engineering Sciences Vol. 41, No. 4, 2013.

[21]. Shamshirgar, S. S., Golkhah, M., Rahmati, H., Nekoui, M. A. "Application and Comparison of LQR and Robust Sliding Mode Controllers to Improve Power System Stability" Environmental and Electrical Engineering International Conference, EEEIC. 10-13 May 2009

[22]. Kim, S., and Williamson, S. S. "Negative Impedance Instability Compensation in More Electric Aircraft DC Power Systems using State Space Pole Placement Control" Vehicle Power and Propulsion Conference (VPPC), IEEE, 2011.

[23]. Emadi, A., Khaligh, A., Rivetta, C.H., and Williamson, G.A., "Constant Power Loads and Negative Impedance Instability in Automotive Systems: Definition, Modeling, Stability, and Control of Power Electronic Converters and Motor Drives" IEEE Transactions on Vehicular Technology, Vol. 55, No. 4, July 2006

[24]. Ederhoff, K.B. "Power System Calculations – Part II" Web document. Retrieved from http://www.hv-eng.com/2010IASSymComp.pdf on 05/18/2014

[25]. Li, X. "Stability Analysis and Control Design for Hybrid AC-DC More-Electric Aircraft Power Systems" Diss. University of Pittsburgh, 2013.